ACS OMEGA

Article

Cite This: ACS Omega 2019, 4, 10231−10242

http://pubs.acs.org/journal/acsodf

Compartmentalization of Alkaline-Earth Metals in Salen-Type Cu- and Ni-Complexes in Solution and in the Solid State

Alba Finelli,[†] Nelly Hérault,[†] Aurélien Crochet,[‡] and Katharina M. Fromm*[,†]

[†]Department of Chemistry and [‡]FriMat, Department of Chemistry, University of Fribourg, Ch. du Musée 9, 1700 Fribourg, Switzerland

Supporting Information

ABSTRACT: The precise arrangement of metal ions in type and number by a ligand represents an important challenge in biology as well as in materials science. The preorganization of different metal ions such as alkaline-earth and transition-metal ions is of particular interest for the design of catalysts or precursors of oxides. This study is based on a Ω-shaped salen-derived ligand comprising N_2O_2 and O_2O_2 coordination sites. The selective binding of Cu(II) and Ni(II) and alkaline-earth-metal ions is influenced by many factors such as the size of the cation, the solvent, or the counterion. UV−vis and ^{1}H NMR titrations and single-crystal X-ray structures reveal that the obtained complexes tend to adopt different structures in solution compared to the solid state. Mainly discrete motifs with a stoichiometry 1:1 (LM_1 to alkaline-earth-metal ions) have been shown to form in the solid state, whereas in solution, the 2:1 complexes are predominant.

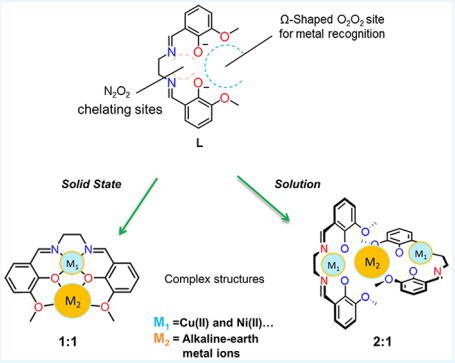

INTRODUCTION

The design and synthesis of new mixed transition-metal and alkaline-earth-metal complexes is of interest in many fields such as catalysis,[1−3] material sciences,[4−10] or biochemistry.[11−14] Furthermore, their abundance, their affordability, and in most cases their biocompatibility represent a real advantage. However, research on alkaline-earth-metal materials represents a considerable challenge[15] due to the lack of preferred geometrical coordination and coordination numbers resulting from their large ionic radii and electronic configuration.[16−21]

Interesting and enhanced properties for potential biological or physical applications can emanate from the combination and the complexation of specific metal ions[22−26] orderly placed in different compartments of one ligand entity, delivering various intriguing structural architectures.[27−33] For instance, aluminum−dipyrrin complexes able to selectively bind alkaline-earth ions in an aqueous mixed solvent have been recently synthesized and can be applied for colorimetric and/or fluorometric sensing applications.[34−37]

Compartmentalized multimetallic compounds are also of particular interest as precursors for the production of mixed metal oxides[38−43] via the single-source precursor method.[44,45] Although diketonates[46−48] and ketoimines[49,50] are the typical ligands for binding alkaline-earth ions, a multitopic polyether-based ligand with specific chelating sites has been designed, allowing the selective coordination of Cu(II) in one site and Ba(II) or Ca(II) in a second site.[51] The obtained heterometallic complexes were further thermally decomposed to stoichiometric mixed metal compounds. The choice of a versatile organic ligand with specific coordination sites is thus of crucial importance for the synthesis of such compounds.[32,52]

Since the past few years, several research groups have carried out numerous studies on multi-metal-containing host−guest complexes based on salen-type ligands.[53,54,63−69,55−62] However, even though transition-metal ions have been widely used in combination with salen-derived ligands for multiple purposes, systems with alkaline-earth-metal ions were poorly investigated.[52,70]

In a previous work,[71] we have explored the heterometallic systems derived from a 3-methylsalicylaldehyde-diamine ligand (H_2L) containing two specific coordination sites.[72,73] Its central coordination site was composed of an imine-based N_2O_2 entity coordinating either Cu(II) or Ni(II) ions. The subsequent prearrangement of the ligand into a Ω-shape generated a second recognition site, O_2O_2, composed of two phenoxy and two methoxy groups able to coordinate hard alkali-metal ions. Our copper- and nickel-based metalloligands (LCu or LNi), which showed to be interesting chelate ligands for the uptake[74] of large cations, led us to explore their structural differences upon coordination to group 2 metal ions.

In this research, we report the synthesis and the structural characterization of eight new mixed metal complexes corresponding to the coordination of the alkaline-earth series by LCu and LNi. Different coordination modes can be expected in solution and/or in the solid state[75,76] depending on the size of the metal ion coordinated at the O_2O_2 site. The

Received: February 18, 2019
Accepted: April 25, 2019
Published: June 13, 2019

DOI: 10.1021/acsomega.9b00365
ACS Omega 2019, 4, 10231−10242

structural studies of alkali complexes described in our previous work, combined with the herein described study of alkaline-earth compounds in both solution and the solid states, constitute a great leap forward in the understanding of the salen-based complex chemistry in crystal engineering and provide valuable details on the compartmentalization of alkali-, alkaline-earth-, and transition-metal ions.

RESULTS AND DISCUSSION

The ligand H_2L (Scheme 1) was synthetized by a straightforward nucleophilic addition from *o*-vanillin and ethane-1,2-diamine forming a hemiaminal, based on a literature procedure.[72] Copper(II) or nickel(II) metal ions selected as M_1 have been coordinated to the deprotonated H_2L ligand (L^{2-}). Indeed, the copper ion is preferentially coordinated in a square pyramidal coordination, whereas the nickel ion tends to adopt a quasiperfect square planar configuration. The structural differences influenced by the uptake of the alkaline-earth-metal ions between the nickel(II) and the copper(II) complexes have been studied.

Scheme 1. Synthesis of H_2L and Its Two Potential Coordination Sites after Deprotonation

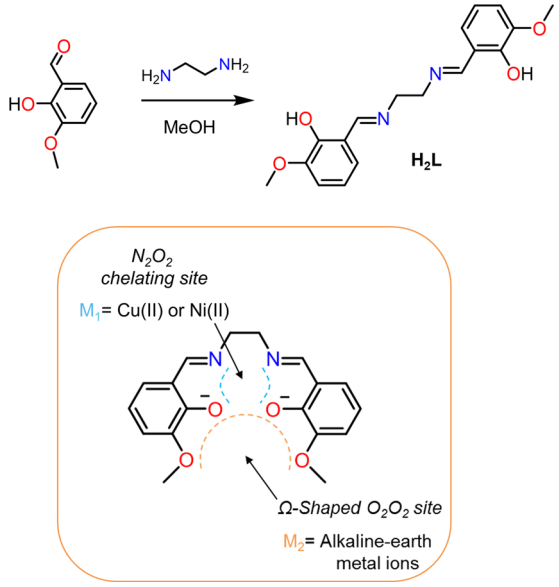

Binding of Alkaline-Earth-Metal Ions to the O_2O_2 Recognition Site: Solution Studies. The metalloligands LM_1 [M_1 = Cu(II) or Ni(II)] were studied upon the addition of the alkaline-earth-metal ion M_2, performing ^{1}H NMR and UV−vis titrations. The second metal ion insertion was investigated by mixing LCu or LNi with the alkaline-earth-metal salts. In a solvent mixture of ACN/EtOH, stoichiometric amounts were reacted for 2 h at room temperature (RT). ^{1}H NMR studies have been performed on LNi ligands to investigate the formation of the different heterometallic compounds in solution as the complexes are diamagnetic, whereas UV−vis measurements have been performed on LCu-derived compounds as the Cu(II) compounds are paramagnetic, hence NMR silent, while exhibiting a color change upon addition of the alkaline-earth-metal ion, in contrast to Ni(II) complexes.

^{1}H NMR Study. Upon addition of aliquots of Mg, Ca, and Sr salts to the solution of LNi, broad peaks appeared particularly for the imine and the aromatic signals. This effect can be explained by an intermediate exchange regime ($k \approx \Delta f$), and only one signal is observed with an intermediate chemical shift denoting a moderate affinity at room temperature between the metalloligand and the alkaline-earth-metal ion. The measurements were then performed at 70 °C to increase the exchange rate and observe distinct shifted peaks (Figures S2−S5 and 1). Only the NMR titration with barium was carried out at room temperature to establish the exact stoichiometry of the complex, as the spectrum showed a neat slow exchange regime ($k \ll \Delta f$). High-field shifts of the imine signals were observed when the alkaline-earth-metal salts were added.

The complexation of Mg, Ca, Sr, or Ba with LNi leads to the formation of 2:1 (LNi/M_2 ratio) species in solution where a plateau is reached upon the addition of 0.5 equiv of metal salts confirmed by the maximum value at 0.66 on their corresponding Job plot.

UV−Vis Measurements. The corresponding LCu compounds were analyzed by UV−vis upon the addition of aliquots of the alkaline-earth-metal ion solutions. The measurements were performed in a mixture of acetonitrile and dimethyl sulfoxide (DMSO). The LCu metalloligand showed two characteristic high-intensity bands located below 420 nm and one broad band in the visible region.[77] The strongest band appears at around 280 nm and is assigned to the $\pi \rightarrow \pi^*$ transition resulting from the extended delocalized π-systems of the azomethine group. A band at 360 nm is associated with the metal-to-ligand charge transfer transition. A weak broad d−d transition band located in the visible region is detected at around 550 nm related to the ligand field. During the titrations, a decrease of both intense absorption bands is detected, accompanied by an increase of slightly blue-shifted bands (hypsochromic shift) through two isosbestic points, indicating the transformation of one species into another. The decrease of intensity as well as the slight hypsochromic shift is also observed for the weak visible broad band influenced by the insertion of the second metal ion. The binding isotherm of each titration reaches a plateau at around 0.5 equiv of added alkaline-earth-metal ions, confirming together with their Job plot maximum at 0.66 the formation of a 2:1 complex (Figure 2). (Detailed data on all of the individual titrations can be found in the Supporting Information, Figures S6−S9.)

The titration of LCu with a barium salt shows a different behavior compared to the rest of the alkaline-earth-metal ions. For the larger Ba(II) ion, a plateau is detected upon addition of 0.5 equiv of Ba(II) ions. Upon further addition, a slight increase as well as a blue shift of the bands is observed again. This phenomenon indicates the adoption of a 2:1 species at about 0.5 equiv, before the formation of a 1:1 binding mode.

In solution, 2:1 complexes have been obtained for the complexation of alkaline-earth-metal ions with either LNi or LCu. The only exception was observed for the complexation of barium with LCu.

Description of Solid-State Structures. To explore the way in which LCu and LNi bind to the different alkaline-earth-metal ions, we performed single-crystal X-ray analysis on all compounds, for which single crystals in sufficient quality could be obtained. [$LCuMg(NO_3)_2$] is abbreviated as "LCuMg" (**1**), [$LCuCa(\mu\text{-}NO_3)]_n$ as "LCuCa" (**2**), [$LCuSr(NO_3)_2(H_2O)$] as "LCuSr" (**3**), and [$(LCu)_2Ba(NO_3)_2$] as "LCuBa" (**4**). For the nickel-containing compounds, the nomenclature is the following; "LNiMg" for [$\{LNiMg(NO_3)(H_2O)\}(NO_3)$] (**5**),

DOI: 10.1021/acsomega.9b00365
ACS Omega 2019, 4, 10231−10242

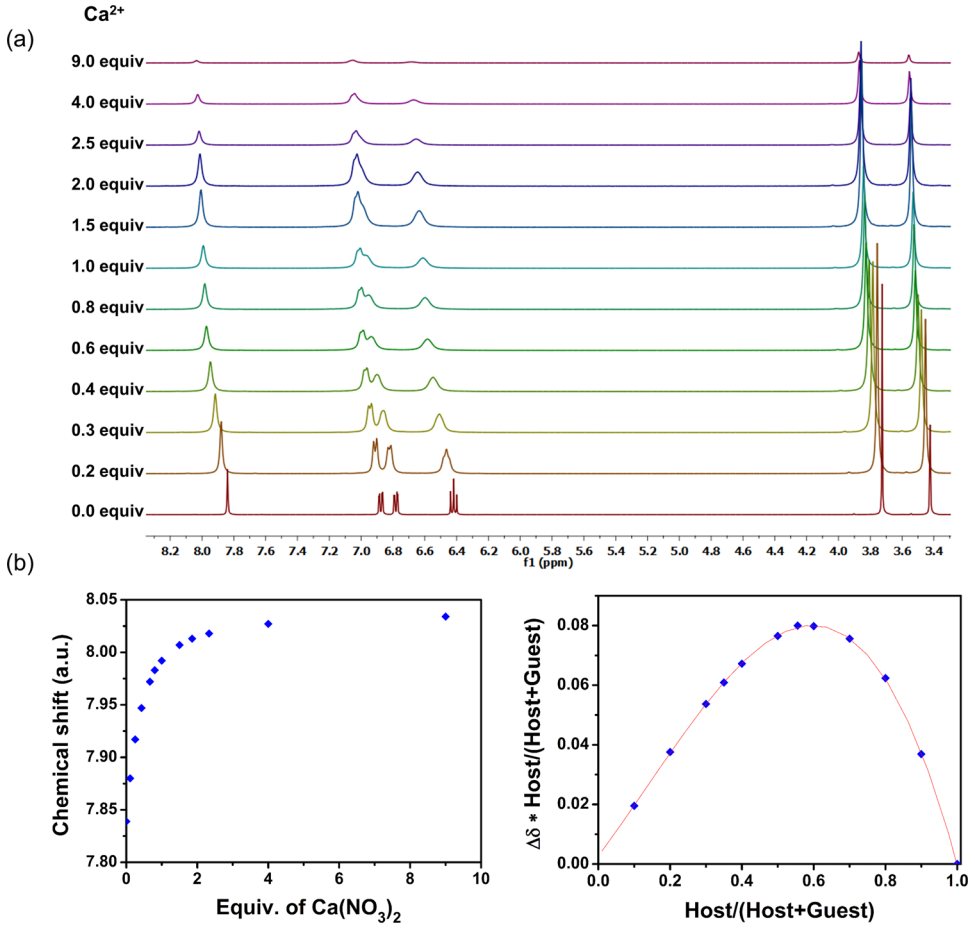

Figure 1. (a) ^{1}H NMR titration of LNi with $Ca(NO_3)_2{\cdot}6H_2O$ forming the corresponding LNiCa complex at room temperature. (b) ^{1}H NMR titration binding isotherm of the LNiCa complex formation focused on the imine proton signal with the Job plot analysis performed with a constant total concentration of [0.04 M].

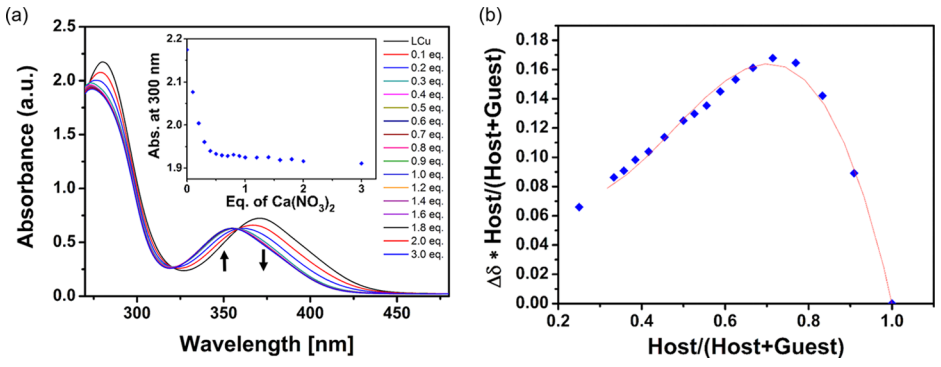

Figure 2. (a) UV−vis titration of LCu with the $Ca(NO_3)_2{\cdot}6H_2O$ complex. Diminution of the absorbance of the two first bands during the titration and appearance of the two isosbestic points and the binding isotherm of LCuCa focused on the second band. (b) Job plot analysis performed with a constant total concentration of [0.0001 M].

"LNiCa" for $[LNiCa(NO_3)_2(H_2O)]$ (**6**), "LNiSr" for $[LNiSr(NO_3)_2(H_2O)]$ (**7**), and "LNiBa" for $[(LNi)_2Ba(NO_3)_2]$ (**8**) (a detailed description of the single-crystal structures of this paper can be found in the Supporting Information, Figures S16−S19, Table S1) (Table 1).

Single crystals of all of the compounds were obtained from the mother liquor of the reaction between LCu or LNi and the corresponding alkaline-earth salts. Each crystal structure presented below shows a 1:1:1 stoichiometry for $L/M_1/M_2$, except for the Ba-compounds, which adopt a 2:2:1 stoichiometry complex. In the following compounds, Cu(II) and Ni(II) are coordinated in a quasiperfect square planar way by the phenolate and imine groups of the N_2O_2 chelating entity of the ligand, with angle sums close to 360°. Similar bond valence sums (BVSs) for M_1 are observed in the series of alkaline-earth-metal compounds, that is, ca. 1.95 in Cu(II) complexes and 2.35 in Ni(II) compounds.[78]

Regarding the O_2O_2 recognition site in compound **1**, Mg(II) is bound to all four O-atoms of the ligand belonging to two phenolate and methoxy groups occupying all of the cavity. The

DOI: 10.1021/acsomega.9b00365
ACS Omega 2019, 4, 10231−10242

Table 1. Crystallographic Data for 1−8

	LCuMg (1)	LCuCa (2)	LCuSr (3)	LCuBa (4)	LNiMg (5)	LNiCa (6)	LNiSr (7)	LNiBa (8)
formula	$C_{18}H_{18}CuMgN_4O_{10}$	$C_{18}H_{18}CuN_4CaO_{10}$	$C_{18}H_{20}CuN_4O_{11}Sr$	$C_{72}H_{72}Ba_2Cu_4N_{12}O_{28}$	$C_{18}H_{20}MgN_4NiO_{11}$	$C_{18}H_{20}CaN_4NiO_{11}$	$C_{18}H_{20}N_4NiO_{11}Sr$	$C_{72}H_{66}Ba_2\ N_{12}Ni_2O_{28}$
M_w	538.21	553.98	619.54	2082.25	551.40	567.17	614.71	2062.85
T [K]	250	200	200	200	200	200	200	250
lattice	triclinic	monoclinic	orthorombic	triclinic	triclinic	monoclinic	orthorombic	triclinic
space group	$P\bar{1}$	$P2_1/n$	$Pna2_1$	$P\bar{1}$	$P\bar{1}$	$P2_1/c$	$Pna2_1$	$P\bar{1}$
a [Å]	7.6984(9)	11.7160(6)	22.7055(5)	11.6329(5)	8.2292(8)	8.4758(4)	22.5345(8)	11.632(2)
b [Å]	10.9592(11)	12.8272(7)	8.6682(5)	16.1304(7)	11.4209(11)	11.1050(4)	8.6074(4)	16.114(3)
c [Å]	12.8941(14)	13.7268(7)	11.1731(14)	23.2105(11)	11.5013(11)	22.9166(11)	11.1107(4)	23.382(6)
α [deg]	90.486(9)	90	90	70.040(4)	83.169(8)	90	90	100.388(17)
β [deg]	97.941(9)	91.441(4)	90	87.041(4)	84.590(8)	99.045(4)	90	92.814(18)
γ [deg]	111.744(8)	90	90	89.654(4)	85.070(8)	90	90	90.137(16)
V [Å^3]	998.7(2)	2062.26(19)	2199.06(3)	4270.1(3)	1065.44(18)	2130.17(16)	2155.07(13)	4305.36
Z	2	4	4	2	2	4	4	2
d_{calc} [g cm^{-3}]	1.790	1.784	1.871	1.619	1.098	1.769	1.895	1.583
R_1/wR_2 [$I > 2\sigma(I)$]	0.0922/0.2230	0.0424/0.1007	0.0395/0.0829	0.0495/0.1069	0.0644/0.1736	0.0353/0.0783	0.0235/0.0506	0.1162/0.2767
Flack parameter			−0.014(5)				−0.015(7)	

coordination sphere of the alkaline-earth cation is completed by three O-atoms of two nitrate anions, leading to a distorted pentagonal bipyramidal arrangement for Mg(II). The bond valence sum provided by O1−O4, O5−O6, and O8 amounts to 1.99, justifying the additional coordination of O6 and hence the unusual coordination number 7 for magnesium.[79−81] The LCuMg entity is not completely planar, as the two aromatic rings form an angle of 4.36°. This is explained by an antiparallel arrangement of the complexes, which leads to alternating parallel strands featuring Cu(II)−C14 interactions [3.318(9) Å] and $\pi-\pi$ interactions along the crystallographic b-axis (Figure 3).

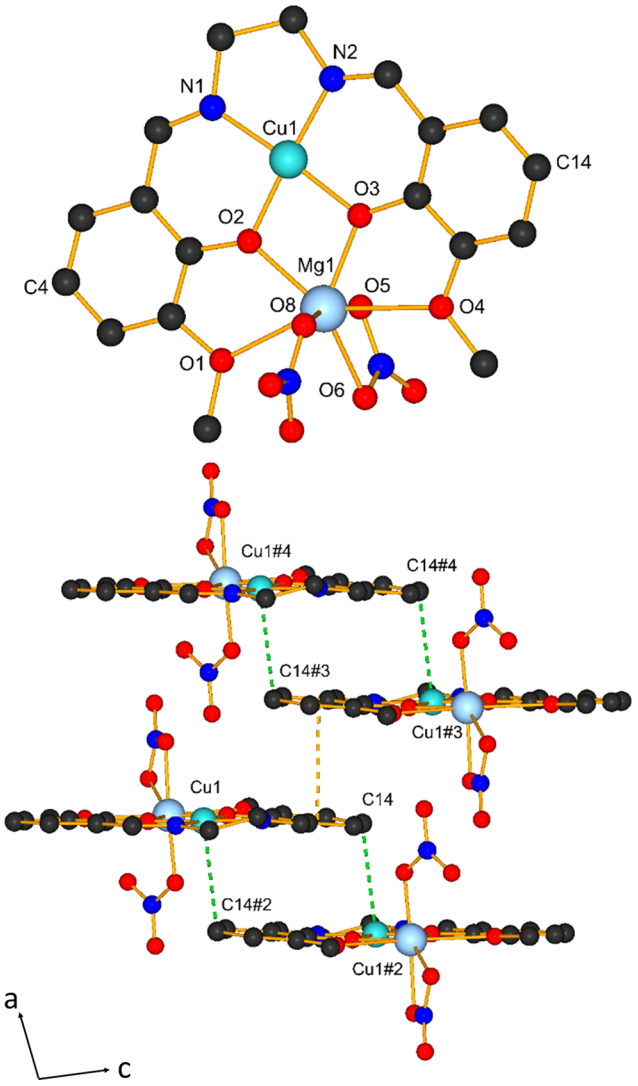

Figure 3. Structure of the asymmetric unit of LCuMg complex **1** (top) and packing thereof [bottom, #2(−x, 1 − y, 1 − z), #3(1 − x, 1 − y, 1 − z), #4(1 + x, y, z)] shows the $\pi-\pi$ interactions (orange dashed bonds) and Cu(II)−C14 interactions (green dashed bonds). H-atoms have been omitted for clarity.

The 1:1 Ni-homologue compound LNiMg (**5**) has a slightly different structure than LCuMg, as Mg(II) is now perfectly accommodated in the quasiplanar ligand (Figure 4). As a major difference, the Mg(II) ion in **5** completes its coordination sphere with two O-atoms of one nitrate anion, O5 and O6, and one molecule of water, O8. This particularity

DOI: 10.1021/acsomega.9b00365
ACS Omega 2019, 4, 10231−10242

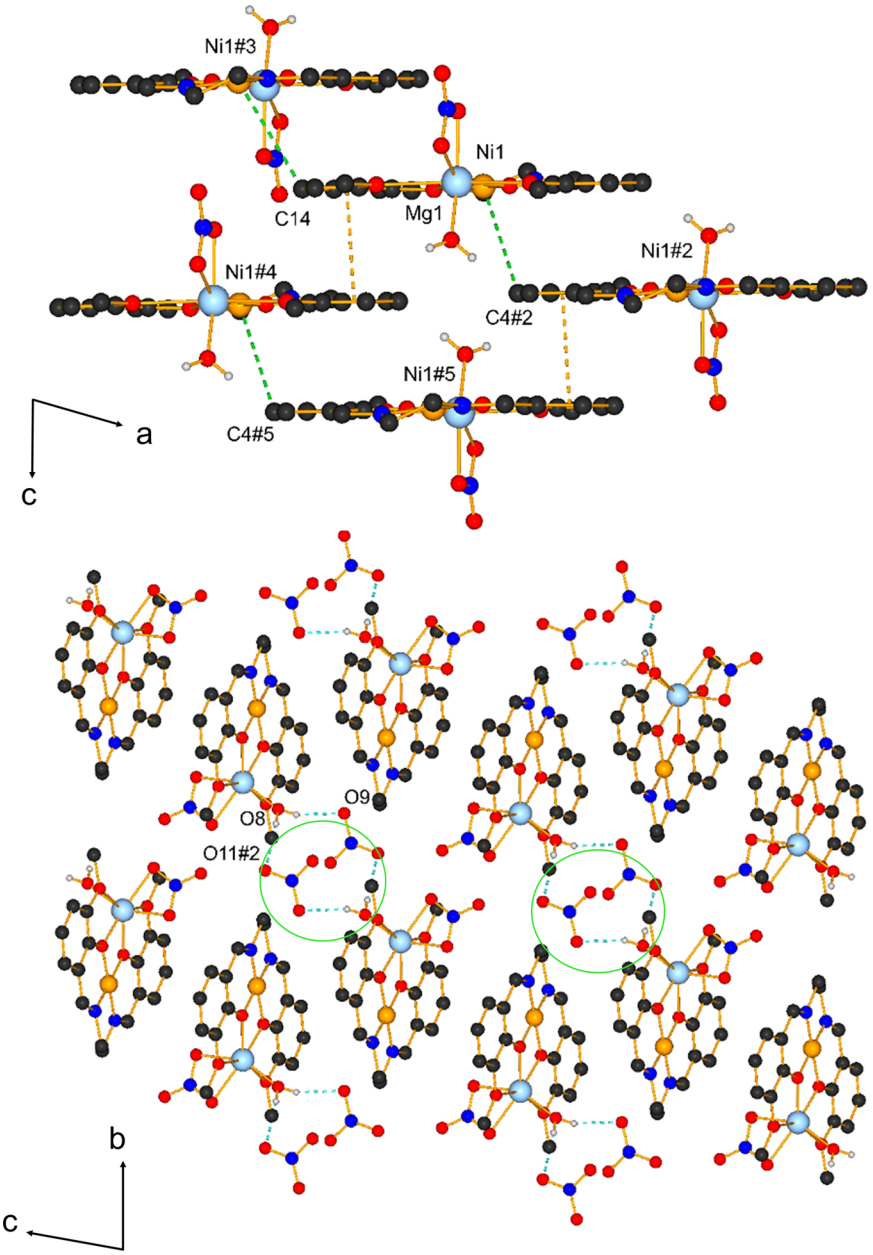

Figure 4. Antiparallel stacking of LNiMg complex **5** [top, #2(2 − *x*, 1 − *y*, 1 − *z*), #3(1 − *x*, 1 − *y*, −*z*), #4(−1 + *x*, *y*, *z*), #5(1 − *x*, 1 − *y*, 1 − *z*)] showing the Ni(II)−C4 and Ni(II)−C14 bonds (green dashed bonds), *π*−*π* packing (orange dashed bonds), and the channels (bottom, green circles); H-bonds (bottom, blue dashed bonds) between different layers create channels along the *a*-axis and comprise two nitrate ions. All H-atoms, except for the water molecules, have been omitted for clarity.

produces two H-bonds between O8 and one O-atom, O9, of a noncoordinated nitrate ion and an O-atom, O11, of a neighbor complex, with 2.753(6) and 2.840(6) Å, respectively. These H-bonds generate a channel along the crystallographic *a*-axis, containing the two anions. The remaining packing resembles the LCuMg pattern with strands of antiparallel packed complexes formed by *π*−*π* packing between the ligands along the crystallographic *b*-axis as well as Ni(II)−C14 and Ni(II)−C4 interactions.

In compound LCuCa (**2**), the calcium ion is coordinated to all four oxygen atoms of the O_2O_2 compartment of the ligand, as well as to five O-atoms stemming from three different nitrate anions. With a bond valence sum (BVS) provided by O1−O4, O5−O6, and O8−O9 of 1.91, the calcium ion completes its coordination sphere with an additional neighboring nitrate O-donor atom (O7) reinforcing its charge resulting in a BVS of 2.15.[79,82] The calcium ion exhibits hence an unusual coordination number of 9, adopting a distorted tricapped trigonal prismatic coordination sphere. One nitrate anion binds via two O-atoms and acts as a terminal ligand, whereas another acts as a bridging ligand and uses all of its O-atoms to coordinate, whereby two O-donors bind to one Ca(II) ion and the third connects to the alkaline-earth-metal ion of the next complex entity. Hence, a one-dimensional (1D) coordination polymer along the *b*-axis with an antiparallel arrangement of the ligands is obtained. This head-to-tail configuration is explained by the consideration of a weak bond between Cu(II) and O6 with 2.675(4) Å. Furthermore, a weak contact between Cu1 and C14 of a neighboring *π*-system with 3.621(5) Å induces a bending of the corresponding aromatic ring of ca.

DOI: 10.1021/acsomega.9b00365
ACS Omega 2019, 4, 10231−10242

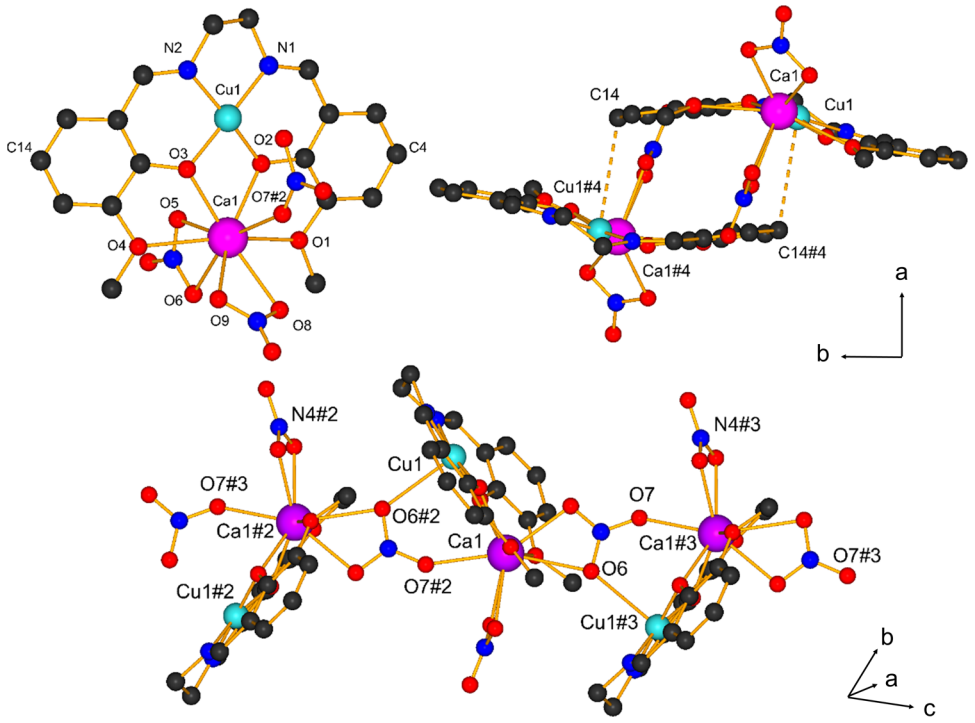

Figure 5. Crystal structure of LCuCa complex **2** (top left, asymmetric unit) reveals a 1D coordination polymer [#2(1/2 − *x*, 1/2 + *y*, 1/2 − *z*), #3(1/2 − *x*, −1/2 + *y*, 1/2 − *z*), #4(1 − *x*, 1 − *y*, −*z*)] by coordination of the calcium ion with the neighboring O7 of a nitrate anion and the Cu(II)−O6 weak bonds (bottom). Distortion of the ligand via Cu(II)−C14 interactions (top right, orange dashed bonds, bottom). H-atoms have been omitted for clarity.

1.795 Å out of the plane formed by the Cu−N_2O_2 entity toward the calcium ion and results in nonplanarity of the ligand with an angle of ca. 16.5° between the two aromatic planes. The calcium ion is thus slightly pulled out of the main plane of the ligand by roughly 0.65 Å (Figure 5).

The complex LNiCa (**6**), as well as LCuSr (**3**) and its nickel homologue compound LNiSr (**7**), adopts a similar structural motif as the compound LCuMg (**1**), except for the fact that the alkaline-earth-metal ion bears an additional water molecule in its coordination sphere, leading to the coordination number 9 for the group 2 ion (Figure 6). The water molecule is arranged approximately in the same plane as the O_2O_2 entity of the ligand. As in **4**, the water molecule O11 produces two H-bonds via the two nitrate oxygen atoms, O7 and O8. The arrangement in the unit cell is governed by $\pi-\pi$ packing interactions between two parallel neighbor units expanding in a stairlike motif along the *b*-axis. An antiparallel arrangement of ligand π−system interactions completes this expansion via Cu(II)−C4 interactions. Compared to compound LCuMg (**1**), this motif is altered by the presence of H-bonds, which allows this exact pattern to be reproduced along the *b*-axis forming alternating layers.

The complexation of barium with LCu and LNi leads to the formation of 2:1 complexes LCuBa (**4**) and LNiBa (**8**), which are unique in this series of solid-state structures (Figure 7). The barium cation is too large to fit into the O_2O_2 compartment of the ligand; hence, a sandwich-type structure is preferred. Due to its large ionic radius, the barium ion is able to accommodate two ligands forming a sandwich complex using all O-atoms of the ligands. The asymmetric unit is composed of two sandwich entities. The metalloligands of one complex are parallel to each other, exhibiting an offset angle of ca. 48° for the Ba1 complex and 47° for the Ba2 complex. In addition, four O-atoms of two nitrate ions coordinate to Ba1, whereas only three O-atoms of two nitrate moieties bind to Ba2. This leads to a coordination number of 12 for Ba1 and 11 for Ba2, with BVS of 2.21 and 2.25, respectively. The two independent complexes form an angle of ca. 74° with respect to each other and are linked to symmetry equivalents via Cu(II)−π interactions along the *a*-axis.

Overall, the solid-state structures reveal predominantly complexes with 1:1 stoichiometry, except LCuBa (**4**) or LNiBa (**8**), which form sandwich-type arrangements. Indeed, a larger cation like barium cannot be accommodated in the mean plane of the O_2O_2 cavity; hence, a sandwich-type structure is preferred. As observed in our previous studies,[71] alkali metal ions with ionic radii bigger than ca. 135 pm (Ba^{2+} = 135 pm, K^+ = 138 pm, Rb^+ = 158 pm, Cs^+ = 167 pm) are generally pushed out of the M_1-N_2O_2 main plane forming eventually coordination polymers or sandwich configurations. Andruh et al.[83,84] and Costes et al.[85] have obtained several complexes based on *o*-vanilin and composed of Cu(II) or Ni(II) combined with Ln(III), where M_2 tends to be located out of the M_1-N_2O_2 plane. Indeed, the use of longer amine chains in the ligand synthesis allows a higher degree of freedom to the transition-metal coordination in the N_2O_2 chelating moiety, leading to a greater scaffold distortion. Compounds LCuSr (**3**), LNiMg (**5**), LNiCa (**6**), and LNiSr (**7**) bear one water molecule, allowing the generation of H-bonds, which induces the formation of alternating layers. While all of the remaining 1:1 structures follow a similar packing pattern via M−C as well as $\pi-\pi$ interactions, LCuCa (**2**) adopts a one-dimensional coordination polymer structure by involving a bridging nitrate anion.

The alkaline-earth and alkali complexes[71] exhibit different structural trends. While the LCu−alkali complexes are

DOI: 10.1021/acsomega.9b00365
ACS Omega 2019, 4, 10231−10242

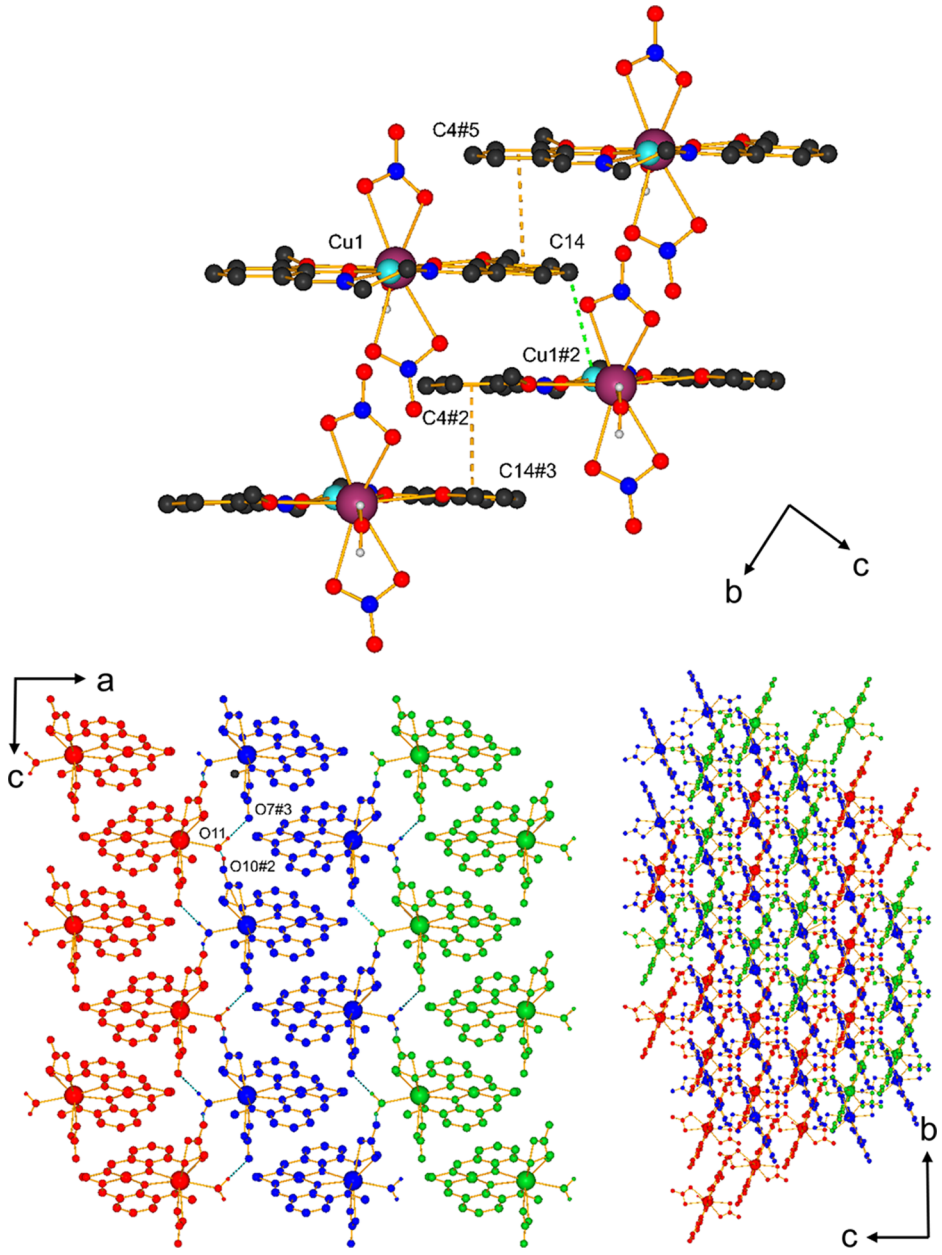

Figure 6. Crystal structure of LCuSr complex **3** [top, #2(x, $-1 + y$, z), #3($1/2 - x$, $-1/2 - y$, $1/2 + z$), #5($1/2 - x$, $1/2 + y$, $-1/2 + z$)] presenting similar characteristics as compounds LNiCa (**6**) and LNiSr (**7**). They show an antiparallel arrangement of complexes via Cu(II)−C14 (green dashed bonds) and $\pi-\pi$ interactions (orange dashed bonds, top). The presence of H-bonds creates different layers shown from the top and from the profile (bottom, blue dashed bonds, bottom). All H-atoms, except for water molecules, have been omitted for clarity.

arranged in an antiparallel fashion to form 1D coordination polymers most of the time, the LNi−alkali compounds formed polar chains with the ligands pointing to the same side of the coordination polymer chain. This could be explained by the fact that Cu(II) was less well coordinated by the N_2O_2 moiety (BVS < 2) than Ni(II) and interacted thus more strongly with counterions, whereas in the Ni(II) compounds, the metal−π interactions dominated. For the herein presented alkaline-earth-metal complexes of LCu and LNi, no clear trend in the packing of the complex moieties can be observed, despite the comparable trend in the bond valence sum. Cu(II) seems "satisfied" with its coordination and does not "seek" further ligands, as exemplified by only weak contacts to carbon atoms of neighbor aromatic rings. One reason for this may be based on the fact that the alkaline-earth-metal cations are smaller and charged 2+, fitting better into the O_2O_2 cavity compared to the alkali-metal homologues. Indeed, the coordination of larger cations like alkali-metal ions causes a slight deformation of the ligand scaffold, leading to a change in the aromaticity. This effect promotes thus close interactions between Cu(II) and additional neighboring O-atoms to satisfy the charge of the copper. Another difference compared to the alkali-metal compounds is the coordination of a water molecule to the alkaline-earth-metal ions in most of the herein shown cases, leading to H-bonds among the different complexes. Finally, the alkaline-earth-metal complexes of LCu and LNi require two counterions to balance the charge. These counterions are in many cases placed in axial positions with respect to the ligand donor atoms and repel each other between two neighbor complexes, leading to antiparallel arrangements. Overall, the

DOI: 10.1021/acsomega.9b00365
ACS Omega 2019, 4, 10231−10242

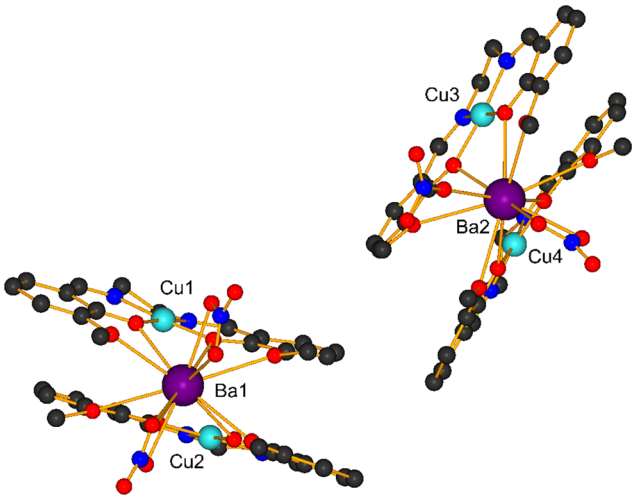

Figure 7. Crystal structure of the sandwich arrangement of LCuBa complex **4**. All H-atoms have been omitted for clarity.

alkaline-earth-metal ions are also well shielded by the coordinating entities and do not possess free space for further, eventually, bridging coordination, except for compound LCuCa (**2**), where no water molecule is bound, leaving space for an additional O-atom that comes from a bridging nitrate ion. Thus, the Ca(II) ion is displaced out of the main plane of the ligand with a distance of ca. 0.65 Å, distorting the LCu ligand with an angle of ca. 16.5°. This effect induces hence a slight disturbance of the aromaticity and a close interaction between Cu(II) and the O-atom of a nearby nitrate ion generating this head-to-tail arrangement of the polymer. We thus tried to obtain all compounds in their water-free form, but the resulting material is amorphous or does not crystallize well enough to determine their structure.

CONCLUSIONS

New alkaline-earth-metal-containing complexes derived from a salen-based ligand beforehand coordinated to M_1 = Cu(II) or Ni(II) have been studied. The coordination of the N_2O_2 recognition site of the ligand H_2L to M_1 generates a Ω-shaped O_2O_2 chelating site able to host alkaline-earth-metal ions M_2. The M_2 recognition was explored in solution by UV−vis and ^{1}H NMR titrations at different temperatures and showed an evident presence of 2:1 (LM_1/M_2) compounds, upon the addition of different alkaline-earth salts. A 2:1 stoichiometry complex in solution has been confirmed, whereas in most cases, one single stoichiometry was favored in the solid state. The X-ray crystallographic measurements of the different alkaline-earth complexes exhibit a neat tendency toward a 1:1:1 ($L/M_1/M_2$) composition, except for Ba(II). The compounds corresponding to the 2:1 ratio might indicate the presence of oligomers stemming from a coordination polymer. The main difference between the alkali and alkaline-earth complexes is that no typical arrangement was detected according to the use of different transition-metal ions in this work. Although having bond valence values similar to those of the alkali-containing complexes, Cu(II) does not seek further ligands to complete its coordination sphere as seen in the alkali study. This may be explained by the fact that the alkaline-earth-metal cations are smaller and charged 2+, fitting better into the O_2O_2 compartment and two axially binding anions. The binding capability of salen-type compounds and the combination of two distinct metal ions within one ligand represent an important benefit in diverse research fields. Especially, the elaboration of new mixed oxide material precursors as well as optical probe compounds is actually ongoing in our group.

EXPERIMENTAL SECTION

General. All experiments were performed in air at RT. Both complex ligands LCu and LNi were prepared as described in the literature.[86,87] All chemicals were commercial products of reagent grade and were used without further purification. ^{1}H and ^{13}C measurements were performed for the Ni(II) compounds with a Bruker 400 MHz NMR spectrometer at RT, and chemical shifts are given in parts per million with respect to the residual solvent peak. Mass spectra (electrospray ionization (ESI)-time-of-flight, positive mode) were recorded with a Bruker Esquire HCT spectrometer with a DMF/ACN mixture as the solvent. For each compound, the bimetallic complexes with a counterion have been observed due to the ionization. The UV/vis spectra were recorded for Cu complexes with a Perkin-Elmer Lambda 40 spectrometer. Powder X-ray diffraction investigations were carried out on a Stoe STADI P diffractometer with CuK (λ = 1.5406 Å) radiation. In most cases, the powder X-ray spectrum of each bulk compound corresponds well to the respective single-crystal data; a high background also indicates amorphous contributions that might slightly falsify the data of the elemental analyses (X-ray powder diffraction (PXRD) diffractograms can be found in the Supporting Information, Figures S10−S15, except for LCuMg (**1**) and LNiBa (**8**) due to a strong amorphous contribution). Elemental analyses for C, H, and N were carried out using a FLASH 2000 Organic Elemental Analyzer. The elemental analysis relative to LNiBa (**8**) compound has not been shown in this work due to the possible interferences with the metals during the mineralization. The precipitates for each compound were dried and measured. However, some of the results show the residual solvent or water molecule. Powder X-ray diffraction investigations were carried out on a Stoe STADI P diffractometer with CuK (λ = 1.5406 Å) radiation. In most cases, the powder X-ray spectrum of the precipitate compound corresponds well to the respective single-crystal data; a high background also indicates amorphous contributions that might slightly falsify the data of the elemental analyses (PXRD diffractograms can be found in the Supporting Information, Figures S10−S15, except for LCuMg (**1**) and LNiBa (**8**) due to a strong amorphous contribution). The crystallographic data of single crystals were collected with Mo Kα radiation (λ = 0.71073 Å). The measurements were performed at 200 and 250 K for the compounds **5** and **8**, with Stoe IPDS-II or IPDS-II T diffractometers equipped with Oxford Cryosystem open-flow cryostats.[88] Single crystals were placed in an inert oil, picked under the microscope, and mounted on loops. All geometric and intensity data were collected from one single crystal. The absorption corrections were partially integrated in the data reduction procedure.[89] The structures were solved and refined using full-matrix least squares on F^2 with the SHELX-2014 package.[90] All atoms, except hydrogen atoms, were refined anisotropically. Hydrogen atoms were refined where possible and otherwise added using the riding model position parameters. Crystallographic data can be found in the Supporting Information (see Table S1). CIF files can be obtained from the Cambridge Crystallographic Data Centre: CCDC-1860971 (**1**), CCDC-1860972 (**2**), CCDC-1860973

DOI: 10.1021/acsomega.9b00365
ACS Omega 2019, 4, 10231−10242

(3), CCDC-1860974 (4), CCDC-1860975 (5), and CCDC-1860976 (6), CCDC-1860977 (7), and CCDC-1860978 (8).

Synthesis of Complexes [LCu(H_2O)] "LCu" and LNi. The complexes LCu and LNi were prepared by adaptation of a literature procedure.[86,87]

Synthesis of the Magnesium Complex [LCuMg(NO_3)$_2$] LCuMg (1). A solution of $Mg(NO_3)_2{\cdot}6H_2O$ (65.76 mg, 0.256 mmol) was added to a solution of LCu (100 mg, 0.256 mmol), previously dissolved in a mixture of acetonitrile/ethanol (7:3, 30 mL). The reaction mixture turned dark purple immediately. After being stirred for 2 h at room temperature, the solvent of the resulting solution was removed under reduced pressure to produce a powder of the complex **1** (110 mg, 79.83%). X-ray-suitable single crystals were obtained by dissolving (**1**) in a mixture of acetonitrile/ethanol (7:3, 30 mL), which was allowed to evaporate at room temperature for 1 week; purple, needlelike single crystals were obtained. ESI-MS (m/z): 475.02 $[M - NO_3]^+$, where M corresponds to $LCuMg(NO_3)_2$. Anal. calcd for $C_{18}H_{22}CuMg\ N_4O_{12}$ corresponding to LCuMg (**1**) containing two H_2O molecules: C, 37.65; H, 3.86; N, 9.76%. Found: C, 36.89; H, 2.96; N, 9.40%.

Synthesis of the Calcium Complex [LCuCa(μ-NO_3)]$_n$ LCuCa (2). A solution of $Ca(NO_3)_2{\cdot}4H_2O$ (60.45 mg, 0.256 mmol) was added to a solution of LCu (100 mg, 0.256 mmol), previously dissolved in a mixture of acetonitrile/ethanol (7:3, 30 mL). The reaction mixture turned dark purple immediately. After being stirred for 2 h at room temperature, the resulting solution was partially evaporated and the product was precipitated with diethyl ether. The precipitate was collected by filtration and dried under vacuum to produce the complex **2** (105 mg, 74.03%). The filtrate was allowed to stand at room temperature for 1 week after partial evaporation of the solvent; dark green, needlelike single crystals suitable for X-ray crystallographic analysis were obtained. ESI-MS (m/z): 491.00 $[M - NO_3]^+$, where M corresponds to $LCuCa(NO_3)_2$. Anal. calcd for $C_{18}H_{18}CaCuN_4O_{10}$ (**2**): C, 39.03; H, 3.28; N, 10.11%. Found: C, 39.72; H, 2.00; N, 10.48%.

Synthesis of the Strontium Complex [LCuSr(NO_3)$_2$(H_2O)] LCuSr (3). A solution of $Sr(NO_3)_2$ (54.17 mg, 0.256 mmol) was added to a solution of LCu (100 mg, 0.256 mmol) in a mixture of acetonitrile/ethanol (7:3, 30 mL). The mixture turned red immediately, and the reaction mixture was stirred for 2 h at room temperature. The precipitate was collected by filtration and dried under vacuum to produce the complex **3** (96 mg, 62.34%). Red rhombohedral-like single crystals were obtained by vapor phase diffusion of diethyl ether into the mother liquor of the reaction in a long tube. ESI-MS (m/z): 538.94 $[M - NO_3]^+$, where M corresponds to $LCuSr(NO_3)_2$. Anal. calcd for $C_{18}H_{18}CuN_4O_{10}Sr$ (**3**) without H_2O molecules: C, 35.94; H, 3.02; N, 9.31%. Found: C, 34.54; H, 1.86; N, 9.51%.

Synthesis of the Barium Complex [(LCu)$_2$Ba(NO_3)$_2$] LCuBa (4). A solution of $Ba(NO_3)_2$ (66.90 mg, 0.256 mmol) was added to a solution of LCu (100 mg, 0.256 mmol) in a mixture of acetonitrile/ethanol (7:3, 30 mL). The mixture turned red immediately, and after being stirred for 2 h at room temperature, the resulting solution was partially evaporated and the product was precipitated with diethyl ether. The precipitate was collected and dried under vacuum to afford the complex **4** (112 mg, 42.02%). After a few days, red needlelike single crystals suitable for X-ray crystallographic analysis were obtained by vapor phase diffusion of diethyl ether into the mother liquor of the reaction in a long tube. ESI-MS (m/z): 978.01. $[M - NO_3]^+$, where M corresponds to $(LCu)_2Ba(NO_3)_2$. Anal. calcd for $C_{36}H_{36}BaCu_2N_6O_{14}$ (**4**): C, 41.53; H, 3.43; N, 8.07%. Found: C, 39.21; H, 3.55; N, 8.11%.

Synthesis of [{LNiMg(NO_3)(H_2O)}(NO_3)] LNiMg (5), [LNiCa(NO_3)$_2$(H_2O)] LNiCa (6), [LNiSr(NO_3)$_2$(H_2O)] LNiSr (7), and [(LNi)$_2$Ba(NO_3)$_2$] LNiBa (8). These compounds were prepared by the same method as described above, by reacting LNi in an acetonitrile/ethanol (7:3) solution with 1 equiv of the appropriate alkaline-earth-metal salt. The metal salts used were as follows: $Mg(NO_3)_2{\cdot}6H_2O$ for **5**, $Ca(NO_3)_2{\cdot}4H_2O$ for **6**, $Sr(NO_3)_2$ for **7**, and $Ba(NO_3)_2$ for **8**.

Data for 5. Yield: 89% (123.27 mg). ^{1}H NMR (400 MHz, DMSO-d_6): δ (ppm) 3.43 (s, 4H), 3.73 (s, 6H), 6.40−6.44 (t, J = 7.8 Hz, 2H), 6.77−6.79 (dd, J = 7.6, 1.5 Hz, 2H), 6.87−6.90 (dd, J = 8, 1.6 Hz, 2H), 7.85 (s, 2H). ESI-MS (m/z): 470.03 $[M - NO_3]^+$, where M corresponds to $LNiMg(NO_3)_2$. Anal. calcd for $C_{20}H_{26}MgN_4NiO_{12}$ corresponding to LNiMg (**5**) including one EtOH molecule: C, 40.21; H, 4.39; N, 9.38%. Found: C, 38.58; H, 4.26; N, 8.97%.

Data for 6. Yield: 93% (131.09 mg). ^{1}H NMR (400 MHz, DMSO-d_6): δ (ppm) 3.56 (s, 4H), 3.87 (s, 6H), 6.66−6.69 (t, J = 7.8 Hz, 4H), 7.05−7.07 (dd, J = 8, 1.6 Hz, 2H), 8.03 (s, 2H). ESI-MS (m/z): 486.01 $[M - NO_3]^+$, where M corresponds to $LNiCa(NO_3)_2$. Anal. calcd for $C_{18}H_{18}CaN_4NiO_{10}$ corresponding to LNiSr (**6**) without one H_2O molecule: C, 39.37; H, 3.30; N, 10.20%. Found: C, 39.57; H, 2.89; N, 9.76%.

Data for 7. Yield: 75% (116.20 mg). ^{1}H NMR (400 MHz, DMSO-d_6): δ (ppm) 3.46 (s, 4H), 3.8 (s, 6H), 6.66−6.70 (t, J = 7.8 Hz, 2H), 6.97−6.99 (dd, J = 7.6, 1.5 Hz, 2H), 6.97−7.06 (dd, J = 8, 1.6 Hz, 2H), 8.19 (s, 2H). ESI-MS (m/z): 533.96 $[M - NO_3]^+$, where M corresponds to $LNiSr(NO_3)_2$. Anal. calcd for $C_{22}H_{30}N_4NiO_{12}Sr$ corresponding to the LNiSr (**7**) including two EtOH molecules and without one H_2O molecule: C, 38.36; H, 4.39; N, 8.13%. Found: C, 39.26; H, 2.12; N, 8.51%.

Data for 8. Yield: 41% (109.82 mg). ^{1}H NMR (400 MHz, DMSO-d_6): δ (ppm) 3.29 (s, 4H), 3.67 (s, 6H), 6.63−6.67 (t, J = 7.8 Hz, 2H), 6.99−7.01 (dd, J = 7.6, 1.5 Hz, 2H), 7.19−7.21 (dd, J = 8, 1.6 Hz, 2H), 7.84 (s, 2H). ESI-MS (m/z): 968.03 $[M - NO_3]^+$, where M corresponds to $(LNi)_2Ba(NO_3)_2$.

^{1}H NMR Spectroscopy Titration. LNi samples were prepared in deuterated DMSO by varying the $M(NO_3)_2$ stoichiometry from 0 to 2 equiv (M = Mg, Ca, Sr, Ba). Spectra of the nickel complexes were recorded at 70 °C with a 400 MHz NMR spectrometer, except for Ba, whose spectra were recorded at RT. Due to the paramagnetism of the Cu(II) compounds, no ^{1}H NMR measurements were performed on these complexes. A Job plot was performed under the condition where the sum of the concentrations of the host and the guest is constantly [0.04 M] in DMSO. Binding isotherms as well as Job plots were collected, taking the imine peaks as a reference.

UV−Vis Titration. Samples containing 0.1 mM LCu in acetonitrile were prepared (3 mL in the cuvette). Alkaline-earth-metal salts were added from 0 to 3 equiv using 0.03 M solutions of $M(NO_3)$ (M = Mg, Ca, Sr, Ba) in DMSO (addition of 2 μL). Spectra were recorded at RT in a 1 mm path-length quartz cell on a Perkin-Elmer Lambda 40 spectrometer. Job plots were performed where the sum of the concentrations of the host and the guest was [0.0001 M] in a mixture of DMSO and acetonitrile. Binding isotherms as well

DOI: 10.1021/acsomega.9b00365
ACS Omega 2019, 4, 10231−10242

as Job plots were collected, taking a wavelength of 373 nm as a reference.

■ ASSOCIATED CONTENT

Supporting Information

The Supporting Information is available free of charge on the ACS Publications website at DOI: 10.1021/acsomega.9b00365.

CCDC-1860971−18609778 contain the supplementary crystallographic data for this paper (CIF) (CIF) (CIF) (CIF) (CIF) (CIF) (CIF) (CIF) (CIF)

checkCIF/PLATON report; structure factors (PDF)

General; UV−vis titration of the metallohost LCu; NMR spectra of LNi; NMR titration of metallohost LNi; PXRD diffractograms of the alkaline-earth-metal complexes; crystallography (PDF)

■ AUTHOR INFORMATION

Corresponding Author

*E-mail: katharina.fromm@unifr.ch.

ORCID

Alba Finelli: 0000-0002-0273-9613

Nelly Hérault: 0000-0001-8986-7759

Notes

The authors declare no competing financial interest.

■ ACKNOWLEDGMENTS

This work was supported by the Swiss National Science Foundation (Project No. 152777), by Frimat, and by the University of Fribourg.

■ REFERENCES

(1) Kobayashi, S.; Yamashita, Y. Alkaline Earth Metal Catalysts for Asymmetric Reactions. *Acc. Chem. Res.* **2011**, *44*, 58−71.

(2) Harinath, A.; Bhattacharjee, J.; Sarkar, A.; Nayek, H. P.; Panda, T. K. Ring Opening Polymerization and Copolymerization of Cyclic Esters Catalyzed by Group 2 Metal Complexes Supported by Functionalized P−N Ligands. *Inorg. Chem.* **2018**, *57*, 2503−2516.

(3) Gryglewicz, S. Alkaline-Earth Metal Compounds as Alcoholysis Catalysts for Ester Oils Synthesis. *AAppl. Catal., A* **2000**, *192*, 23−28.

(4) Ren, J.; Yang, L.; Qiu, J.; Chen, D.; Jiang, X.; Zhu, C. Effect of Various Alkaline-Earth Metal Oxides on the Broadband Infrared Luminescence from Bismuth-Doped Silicate Glasses. *Solid State Commun.* **2006**, *140*, 38−41.

(5) Fromm, K. M.; Sagué, J. L.; Robin, A. Y. Silver Coordination Polymers with Isonicotinic Acid Derived Short Polyethylene Glycol−Synthesis, Structures, Anion Effect and Solution Behavior. *Inorg. Chim. Acta* **2013**, *403*, 2−8.

(6) Heeger, A. J. Semiconducting and Metallic Polymers: The Fourth Generation of Polymeric Materials (Nobel Lecture). *Angew. Chem., Int. Ed.* **2001**, *40*, 2591−2611.

(7) Wang, Z.; Ye, W.; Luo, X.; Wang, Z. Fabrication of Superhydrophobic and Luminescent Rare Earth/Polymer Complex Films. *Sci. Rep.* **2016**, *6*, No. 24682.

(8) Masoomi, M. Y.; Morsali, A. Applications of Metal−organic Coordination Polymers as Precursors for Preparation of Nano-Materials. *Coord. Chem. Rev.* **2012**, *256*, 2921−2943.

(9) Datta, A.; Das, K.; Massera, C.; Clegg, J. K.; Sinha, C.; Huang, J.-H.; Garribba, E. A Mixed Valent Heterometallic Cu^{II}/Na^{I} Coordination Polymer with Sodium−phenyl Bonds. *Dalton Trans.* **2014**, *43*, 5558−5563.

(10) Zhang, X.; Huang, Y.-Y.; Lin, Q.-P.; Zhang, J.; Yao, Y.-G. Using Alkaline-Earth Metal Ions to Tune Structural Variations of 1, 3, 5-Benzenetricarboxylate Coordination Polymers. *Dalton Trans.* **2013**, *42*, 2294−2301.

(11) Dickson, I. R.; Perkins, D. J. Studies on the Interactions between Purified Bovine Caseins and Alkaline-Earth-Metalions. *Biochem. J.* **1971**, *124*, 235.

(12) Wu, D.; Sedgwick, A. C.; Gunnlaugsson, T.; Akkaya, E. U.; Yoon, J.; James, T. D. Fluorescent Chemosensors: The Past, Present and Future. *Chem. Soc. Rev.* **2017**, *46*, 7105−7123.

(13) He, H.; Rodgers, K. R.; Arif, A. M. Structural and Spectroscopic Studies of Tripodal $[MgL]^{2+}$ Chelates Containing Only Nitrogen Donor Atoms: Alkaline Earth Metal Complexes as Potential Drug Delivery Agents. *J. Inorg. Biochem.* **2004**, *98*, 667−676.

(14) Xu, X.; Hu, F.; Yan, S.; Lin, J.; Li, Q.; Shuai, Q. Eco-Friendly Microwave Synthesis of Mg (II) Phenoxy Carboxylic Acid Coordination Compounds with Specific Motifs Driven by Multiple Hydrogen Bonding. *RSC Adv.* **2016**, *6*, 67610−67618.

(15) Lazarescu, A.; Shova, S.; Bartolome, J.; Alonso, P.; Arauzo, A.; Balu, A. M.; Simonov, Y. A.; Gdaniec, M.; Turta, C.; Filoti, G.; Luque, R. Heteronuclear (Co−Ca, Co−Ba) 2, 3-Pyridinedicarboxylate Complexes: Synthesis, Structure and Physico-Chemical Properties. *Dalton Trans.* **2011**, *40*, 463−471.

(16) Gueneau, E. D.; Fromm, K. M.; Goesmann, H. Synthesis and Structural Analysis of the Polymetallated Alkali Calixarenes [M4 (*p*-*tert*-butylcalix [4] Arene-4H)$(Thf)_x]_2$· *n* THF (M = Li, K; N = 6 or 1; X = 4 or 5) and [Li_2 (*p*-*tert*-butylcalix [4] Arene-2H)(H_2O)(M-H_2O)(Thf)]· 3 THF. *Chem. - Eur. J.* **2003**, *9*, 509−514.

(17) Fromm, K. M.; Gueneau, E. D.; Robin, A. Y.; Maudez, W.; Sague, J.; Bergougnant, R. Recent Advances in the Chemistry of "Clusters" and Coordination Polymers of Alkali, Alkaline Earth Metal and Group 11 Compounds. *Z. Anorg. Allg. Chem.* **2005**, *631*, 1725−1740.

(18) Fromm, K. M.; Gueneau, E. D. Structures of Alkali and Alkaline Earth Metal Clusters with Oxygen Donor Ligands. *Polyhedron* **2004**, *23*, 1479−1504.

(19) Maudez, W.; Fromm, K. M. A Comparative Study of (Poly) Ether Adducts of Alkaline Earth Iodides−An Overview Including New Compounds. *Z. Anorg. Allg. Chem.* **2012**, *638*, 1810−1819.

(20) Yanagida, S.; Takahashi, K.; Okahara, M. Metal-Ion Complexation of Noncyclic Poly (Oxyethylene) Derivatives. I. Solvent Extraction of Alkali and Alkaline Earth Metal Thiocyanates and Iodides. *Bull. Chem. Soc. Jpn.* **1977**, *50*, 1386−1390.

(21) Fromm, K. M. Recent Advances in Tailoring the Aggregation of Heavier Alkaline Earth Metal Halides, Alkoxides and Aryloxides from Non-Aqueous Solvents. *Dalton Trans.* **2006**, 5103−5112.

(22) Lü, X.; Wong, W.; Wong, W. Self-Assembly of Luminescent Platinum-Salen Schiff-Base Complexes. *Eur. J. Inorg. Chem.* **2008**, *2008*, 523−528.

(23) Zhou, H.; Chen, C.; Liu, Y.; Shen, X. Construction of Copper (II)−dysprosium (III)−iron (III) Trinuclear Cluster Based on Schiff Base Ligand: Synthesis, Structure and Magnetism. *Inorg. Chim. Acta* **2015**, *437*, 188−194.

(24) Sarwar, M.; Madalan, A. M.; Tiseanu, C.; Novitchi, G.; Maxim, C.; Marinescu, G.; Luneau, D.; Andruh, M. A New Synthetic Route towards Binuclear 3d−4f Complexes, Using Non-Compartmental Ligands Derived from o-Vanillin. Syntheses, Crystal Structures, Magnetic and Luminescent Properties. *New J. Chem.* **2013**, *37*, 2280−2292.

(25) Modak, R.; Sikdar, Y.; Cosquer, G.; Chatterjee, S.; Yamashita, M.; Goswami, S. Heterometallic Cu^{II}−Dy^{III} Clusters of Different Nuclearities with Slow Magnetic Relaxation. *Inorg. Chem.* **2016**, *55*, 691−699.

(26) Crochet, A.; Brog, J.-P.; Fromm, K. M. Mixed Metal Multinuclear Cr (III) Cage Compounds and Coordination Polymers Based on Unsubstituted Phenolate: Design, Synthesis, Mechanism, and Properties. *Cryst. Growth Des.* **2016**, *16*, 189−199.

(27) Dankert, F.; Donsbach, C.; Mais, C.-N.; Reuter, K.; von Hänisch, C. Alkali and Alkaline Earth Metal Derivatives of Disila-Bridged Podands: Coordination Chemistry and Structural Diversity. *Inorg. Chem.* **2018**, *57*, 351−359.

(28) Hazra, S.; Sasmal, S.; Nayak, M.; Sparkes, H. A.; Howard, J. A. K.; Mohanta, S. Syntheses and Crystal Structures of $Cu^{II}Bi^{III}$, $Cu^{II}Ba^{II}Cu^{II}$,$[Cu^{II}Pb^{II}]_2$ and Cocrystallized $(U^{VI}O_2)_2$. $4Cu^{II}$ Complexes: Structural Diversity of the Coordination Compounds Derived from N, N′-Ethylenebis (3-Ethoxysalicylaldiimine). *CrystEngComm* **2010**, *12*, 470−477.
(29) Sünkel, K.; Nimax, P. R. Structural Diversity in the Alkaline Earth Metal Compounds of Tetra and Pentacyanocyclopentadienide. *Dalton Trans.* **2018**, *47*, 409−417.
(30) Van Veggel, F. C. J. M.; Harkema, S.; Bos, M.; Verboom, W.; Van Staveren, C. J.; Gerritsma, G. J.; Reinhoudt, D. N. Metallomacrocycles: Synthesis, x-Ray Structure, Electrochemistry, and ESR Spectroscopy of Mononuclear and Heterodinuclear Complexes. *Inorg. Chem.* **1989**, *28*, 1133−1148.
(31) Bendjellal, N.; Trifa, C.; Bouacida, S.; Boudaren, C.; Boudraa, M.; Merazig, H. Two Novel Alkaline Earth Coordination Polymers Constructed from Cinnamic Acid and 1, 10-Phenanthroline: Synthesis and Structural and Thermal Properties. *Acta Crystallogr., Sect. C: Struct. Chem.* **2018**, *74*, 240−247.
(32) Carbonaro, L.; Isola, M.; La Pegna, P.; Senatore, L.; Marchetti, F. Spectrophotometric Study of the Equilibria between Nickel (II) Schiff-Base Complexes and Alkaline Earth or Nickel (II) Cations in Acetonitrile Solution. *Inorg. Chem.* **1999**, *38*, 5519−5525.
(33) Zhu, H.-F.; Zhang, Z.-H.; Sun, W.-Y.; Okamura, T.; Ueyama, N. Syntheses, Structures, and Properties of Two-Dimensional Alkaline Earth Metal Complexes with Flexible Tripodal Tricarboxylate Ligands. *Cryst. Growth Des.* **2005**, *5*, 177−182.
(34) Saikawa, M.; Daicho, M.; Nakamura, T.; Uchida, J.; Yamamura, M.; Nabeshima, T. Synthesis of a New Family of Ionophores Based on Aluminum−dipyrrin Complexes (ALDIPYs) and Their Strong Recognition of Alkaline Earth Ions. *Chem. Commun.* **2016**, *52*, 4014−4017.
(35) Wood, T. E.; Thompson, A. Advances in the Chemistry of Dipyrrins and Their Complexes. *Chem. Rev.* **2007**, *107*, 1831−1861.
(36) Baudron, S. A. Luminescent Dipyrrin Based Metal Complexes. *Dalton Trans.* **2013**, *42*, 7498−7509.
(37) Sahana, S.; Bharadwaj, P. K. Detection of Alkali and Alkaline Earth Metal Ions by Fluorescence Spectroscopy. *Inorg. Chim. Acta* **2014**, *417*, 109−141.
(38) Gschwind, F.; Crochet, A.; Maudez, W.; Fromm, K. M. From Alkaline Earth Ion Aggregates via Transition Metal Coordination Polymer Networks towards Heterometallic Single Source Precursors for Oxidic Materials. *Chimia* **2010**, *64*, 299−302.
(39) Brog, J. P.; Crochet, A.; Fromm, K. Lithium Metal Aryloxide Clusters as Starting Products for Oxide Materials, WO2012/000123, 2012.
(40) Wu, M.-K.; Ashburn, J. R.; Torng, C.; Hor, P. H.; Meng, R. L.; Gao, L.; Huang, Z. J.; Wang, Y. Q.; Chu, C. W. Superconductivity at 93 K in a New Mixed-Phase Y-Ba-Cu-O Compound System at Ambient Pressure. *Phys. Rev. Lett.* **1987**, *58*, No. 908.
(41) Ge, H.; Zhang, B.; Gu, X.; Liang, H.; Yang, H.; Gao, Z.; Wang, J.; Qin, Y. A Tandem Catalyst with Multiple Metal Oxide Interfaces Produced by Atomic Layer Deposition. *Angew. Chem.* **2016**, *128*, 7197−7201.
(42) Kung, H. H.; Ko, E. I. Preparation of Oxide Catalysts and Catalyst Supports—a Review of Recent Advances. *Chem. Eng. J. Biochem. Eng. J.* **1996**, *64*, 203−214.
(43) Veith, M. Molecular Precursors for (Nano) Materials—a One Step Strategy. *J. Chem. Soc., Dalton Trans.* **2002**, 2405−2412.
(44) Hubert-Pfalzgraf, L. G. Some Trends in the Design of Homo- and Heterometallic Molecular Precursors of High-Tech Oxides. *Inorg. Chem. Commun.* **2003**, *6*, 102−120.
(45) Elias, J. S.; Risch, M.; Giordano, L.; Mansour, A. N.; Shao-Horn, Y. Structure, Bonding, and Catalytic Activity of Monodisperse, Transition-Metal-Substituted CeO_2 Nanoparticles. *J. Am. Chem. Soc.* **2014**, *136*, 17193−17200.
(46) Gleizes, A.; Sans-Lenain, S.; Medus, D. Structure Cristalline Du Bis (2, 2, 6, 6-Tétraméthyl-3, 5-Heptanedionato) Baryum. *C. R. Acad. Sci., Ser. II: Mec., Phys., Chim., Sci. Terre Univers* **1991**, *313*, 761−766.
(47) Drozdov, A.; Pozhitkov, A.; Troyanov, S.; Pisarevsky, A. Synthesis and X-Ray Structures of Barium Complexes with Pivaloyltrifluoroacetone,$[Ba(Pta)_2(H_2O)]$ and $Ba_4(Pta)_8$. *Polyhedron* **1996**, *15*, 1731−1735.
(48) Hubert-Pfalzgraf, L. G. Metal Alkoxides and B-diketonates as Precursors for Oxide and Non-oxide Thin Films. *Appl. Organomet. Chem.* **1992**, *6*, 627−643.
(49) Schulz, D. L.; Hinds, B. J.; Neumayer, D. A.; Stern, C. L.; Marks, T. J. Barium. Beta.-Ketoiminate Complexes Containing Appended Ether" Lariats". Synthesis, Characterization, and Implementation as Fluorine-Free Barium MOCVD Precursors. *Chem. Mater.* **1993**, *5*, 1605−1617.
(50) Watson, I. M.; Atwood, M. P.; Haq, S. Investigations of Barium Beta-Diketonate Complexes Used in Chemical Vapour Deposition of High-Tc Oxide Films. *Supercond. Sci. Technol.* **1994**, *7*, 672.
(51) Gschwind, F.; Sereda, O.; Fromm, K. M. Multitopic Ligand Design: A Concept for Single-Source Precursors. *Inorg. Chem.* **2009**, *48*, 10535−10547.
(52) Boyle, T. J.; Sears, J. M.; Greathouse, J. A.; Perales, D.; Cramer, R.; Staples, O.; Rheingold, A. L.; Coker, E. N.; Roper, T. M.; Kemp, R. A. Synthesis and Characterization of Structurally Diverse Alkaline-Earth Salen Compounds for Subterranean Fluid Flow Tracking. *Inorg. Chem.* **2018**, *57*, 2402−2415.
(53) Akine, S.; Nabeshima, T. Cyclic and Acyclic Oligo (N_2O_2) Ligands for Cooperative Multi-Metal Complexation. *Dalton Trans.* **2009**, 10395−10408.
(54) Akine, S.; Sairenji, S.; Taniguchi, T.; Nabeshima, T. Stepwise Helicity Inversions by Multisequential Metal Exchange. *J. Am. Chem. Soc.* **2013**, *135*, 12948−12951.
(55) Nabeshima, T.; Akine, S.; Ikeda, C.; Yamamura, M. Metallo-Supramolecular Systems for Synergistic Functions Based on Unique Arrangement of Ligation Sites. *Chem. Lett.* **2010**, *39*, 10−16.
(56) Nakamura, T.; Kimura, H.; Okuhara, T.; Yamamura, M.; Nabeshima, T. A Hierarchical Self-Assembly System Built Up from Preorganized Tripodal Helical Metal Complexes. *J. Am. Chem. Soc.* **2016**, *138*, 794−797.
(57) Hari, N.; Jana, A.; Mohanta, S. Syntheses, Crystal Structures and ESI-MS of Mononuclear−dinuclear, Trinuclear and Dinuclear Based One-Dimensional Copper (II)−s Block Metal Ion Complexes Derived from a 3-Ethoxysalicylaldehyde−diamine Ligand. *Inorg. Chim. Acta* **2017**, *467*, 11−20.
(58) Sasmal, S.; Majumder, S.; Hazra, S.; Sparkes, H. A.; Howard, J. A. K.; Nayak, M.; Mohanta, S. Tetrametallic [2 × 1+ 1 × 2], Octametallic Double-Decker−triple-Decker [5 × 1+ 3 × 1], Hexametallic Quadruple-Decker and Dimetallic-Based One-Dimensional Complexes of Copper (Ii) and s Block Metal Ions Derived from N, N′-Ethylenebis (3-Ethoxysalicylaldimine). *CrystEngComm* **2010**, *12*, 4131−4140.
(59) Sarkar, S.; Mohanta, S. Syntheses, Crystal Structures and Supramolecular Topologies of Nickel(II)−s/p/d^{10}/NH^{4+} Complexes Derived from a Compartmental Ligand. *RSC Adv.* **2011**, *1*, 640−650.
(60) Biswas, A.; Mondal, S.; Mohanta, S. Syntheses, Characterizations, and Crystal Structures of 3d−s/d^{10} Metal Complexes Derived from Two Compartmental Schiff Base Ligands. *J. Coord. Chem.* **2013**, *66*, 152−170.
(61) Constable, E. C.; Zhang, G.; Housecroft, C. E.; Neuburger, M.; Zampese, J. A. Host−guest Chemistry of a Chiral Schiff Base Copper (Ii) Complex: Can Chiral Information Be Transferred to the Guest Cation? *CrystEngComm* **2010**, *12*, 1764−1773.
(62) Frischmann, P. D.; MacLachlan, M. J. Metallocavitands: An Emerging Class of Functional Multimetallic Host Molecules. *Chem. Soc. Rev.* **2013**, *42*, 871−890.
(63) Crane, A. K.; MacLachlan, M. J. Portraits of Porosity: Porous Structures Based on Metal Salen Complexes. *Eur. J. Inorg. Chem.* **2012**, *2012*, 17−30.
(64) Hui, J. K.; Yu, Z.; MacLachlan, M. J. Supramolecular Assembly of Zinc Salphen Complexes: Access to Metal-Containing Gels and Nanofibers. *Angew. Chem., Int. Ed.* **2007**, *46*, 7980−7983.

DOI: 10.1021/acsomega.9b00365
ACS Omega 2019, 4, 10231−10242

(65) Bermejo, M. R.; Carballido, R.; Fernández-García, M. I.; González-Noya, A. M.; González-Riopedre, G.; Maneiro, M.; Rodríguez-Silva, L. Synthesis, Characterization, and Catalytic Studies of Mn (III)-Schiff Base-Dicyanamide Complexes: Checking the Rhombicity Effect in Peroxidase Studies. *J. Chem.* **2017**, *2017*, No. 5465890.
(66) Maneiro, M.; Bermejo, M. R.; Fernandez, M. I.; Gómez-Fórneas, E.; González-Noya, A. M.; Tyryshkin, A. M. A New Type of Manganese-Schiff Base Complex, Catalysts for the Disproportionation of Hydrogen Peroxide as Peroxidase Mimics. *New J. Chem.* **2003**, *27*, 727−733.
(67) Sanmartín, J.; García-Deibe, A. M.; Fondo, M.; Navarro, D.; Bermejo, M. R. Synthesis and Crystal Structure of a Mononuclear Iron (III)(η 2-Acetato) Complex of a β-Cis Folded Salen Type Ligand. *Polyhedron* **2004**, *23*, 963−967.
(68) Kleij, A. W. Zinc-Centred Salen Complexes: Versatile and Accessible Supramolecular Building Motifs. *Dalton Trans.* **2009**, 4635−4639.
(69) Wezenberg, S. J.; Kleij, A. W. Material Applications for Salen Frameworks. *Angew. Chem., Int., Ed.* **2008**, *47*, 2354−2364.
(70) Sánchez, M.; Harvey, M. J.; Nordstrom, F.; Parkin, S.; Atwood, D. A. Salen-Type Compounds of Calcium and Strontium. *Inorg. Chem.* **2002**, *41*, 5397−5402.
(71) Finelli, A.; Hérault, N.; Crochet, A.; Fromm, K. M. Threading Salen-Type Cu-and Ni-Complexes into One-Dimensional Coordination Polymers: Solution versus Solid State, and the Size Effect of the Alkali Metal Ion. *Cryst. Growth Des.* **2018**, *18*, 1215−1226.
(72) Correia, I.; Pessoa, J. C.; Duarte, M. T.; da Piedade, M.; Jackush, T.; Kiss, T.; Castro, M.; Geraldes, C. F. G. C.; Avecilla, F. Vanadium (IV and V) Complexes of Schiff Bases and Reduced Schiff Bases Derived from the Reaction of Aromatic O-Hydroxyaldehydes and Diamines: Synthesis, Characterisation and Solution Studies. *Eur. J. Inorg. Chem.* **2005**, *2005*, 732−744.
(73) Nabeshima, T. Regulation of Ion Recognition by Utilizing Information at the Molecular Level. *Coord. Chem. Rev.* **1996**, *148*, 151−169.
(74) Spisak, S. N.; Wei, Z.; Rogachev, A. Y.; Amaya, T.; Hirao, T.; Petrukhina, M. A. Double Concave Cesium Encapsulation by Two Charged Sumanenyl Bowls. *Angew. Chem.* **2017**, *129*, 2626−2631.
(75) Bhowmik, P.; Chatterjee, S.; Chattopadhyay, S. Heterometallic Inorganic−organic Frameworks of Sodium−nickel (Vanen): Cation−π Interaction, Trigonal Dodecahedral Na^+ and Unprecedented Heptadentate Coordination Mode of Vanen $^{2-}$. *Polyhedron* **2013**, *63*, 214−221.
(76) Hazra, S.; Chakraborty, P.; Mohanta, S. Heterometallic Copper (II)−Tin (II/IV) Salts, Cocrystals and Salt Cocrystals: Selectivity and Structural Diversity Depending on Ligand Substitution and Metal Oxidation State. *Cryst. Growth Des.* **2016**, *16*, 3777−3790.
(77) Tedim, J.; Patrício, S.; Bessada, R.; Morais, R.; Sousa, C.; Marques, M. B.; Freire, C. Third-Order Nonlinear Optical Properties of DA-salen-Type Nickel (II) and Copper (II) Complexes. *Eur. J. Inorg. Chem.* **2006**, *2006*, 3425−3433.
(78) Liu, W.; Thorp, H. H. Bond Valence Sum Analysis of Metal-Ligand Bond Lengths in Metalloenzymes and Model Complexes. 2. Refined Distances and Other Enzymes. *Inorg. Chem.* **1993**, *32*, 4102−4105.
(79) Gschwind, F.; Fromm, K. M. Tetraethylene Glycol Adducts of Alkaline Earth Halides. *Z. Anorg. Allg. Chem.* **2011**, *637*, 1871−1879.
(80) Banerjee, D.; Finkelstein, J.; Smirnov, A.; Forster, P. M.; Borkowski, L. A.; Teat, S. J.; Parise, J. B. Synthesis and Structural Characterization of Magnesium Based Coordination Networks in Different Solvents. *Cryst. Growth Des.* **2011**, *11*, 2572−2579.
(81) Liptrot, D. J.; Hill, M. S.; Mahon, M. F.; MacDougall, D. J. Group 2 Promoted Hydrogen Release from $NMe_2H\cdot BH_3$: Intermediates and Catalysis. *Chem. - Eur. J.* **2010**, *16*, 8508−8515.
(82) Fromm, K. M.; Goesmann, H.; Bernardinelli, G. H-Bonded Polymer Structures of Different Dimensionality: Syntheses and Crystal Structures of $[Ca(DME)_n(H_2O)m]I_2\cdot(DME)_x$ (1: N = 3, M = 3, X = 1; 2: N = 2, M = 4, X = 0) and $[Ca\{CH_3(OCH_2)_3OCH_3\}(H_2O)_4]I_2$. *Polyhedron* **2000**, *19*, 1783−1789.
(83) Visinescu, D.; Alexandru, M.-G.; Madalan, A. M.; Jeon, I.-R.; Mathonière, C.; Clérac, R.; Andruh, M. A New Family of $[Cu^{II}Ln^{III}M^{V}]$ Heterotrimetallic Complexes (Ln = La, Gd, Tb; M = Mo, W): Model Systems to Probe Exchange Interactions and Single-Molecule Magnet Properties. *Dalton Trans.* **2016**, *45*, 7642−7649.
(84) Andruh, M. The Exceptionally Rich Coordination Chemistry Generated by Schiff-Base Ligands Derived from o-Vanillin. *Dalton Trans.* **2015**, *44*, 16633−16653.
(85) Costes, J.-P.; Dahan, F.; Dupuis, A.; Laurent, J.-P. A General Route to Strictly Dinuclear Cu (II)/Ln (III) Complexes. Structural Determination and Magnetic Behavior of Two Cu (II)/Gd (III) Complexes. *Inorg. Chem.* **1997**, *36*, 3429−3433.
(86) Majumder, S.; Koner, R.; Lemoine, P.; Nayak, M.; Ghosh, M.; Hazra, S.; Lucas, C. R.; Mohanta, S. Role of Coordinated Water and Hydrogen-Bonding Interactions in Stabilizing Monophenoxido-Bridged Triangular $Cu^{II}M^{II}Cu^{II}$ Compounds (M = Cu, Co, Ni, or Fe) Derived from N, N′-Ethylenebis (3-methoxysalicylaldimine): Syntheses, Structures, and Magnetic Propert. *Eur. J. Inorg. Chem.* **2009**, *2009*, 3447−3457.
(87) Sarkar, S.; Nayak, M.; Fleck, M.; Dutta, S.; Flörke, U.; Koner, R.; Mohanta, S. Syntheses, Crystal Structures and Mass Spectrometry of Mononuclear Ni^{II} Inclusion Product and Self-Assembled [2 × 1+ 1 × 2] $Ni^{II}{}_3M^{II}$ (M = Cu, Ni, Co, Fe or Mn) Cocrystals Derived from N, N′-Ethylenebis (3-ethoxysalicylaldimine). *Eur. J. Inorg. Chem.* **2010**, *2010*, 735−743.
(88) Cosier, J.; Glazer, A. M. A Nitrogen-Gas-Stream Cryostat for General X-Ray Diffraction Studies. *J. Appl. Crystallogr.* **1986**, *19*, 105−107.
(89) Blanc, E.; Schwarzenbach, D.; Flack, H. D. The Evaluation of Transmission Factors and Their First Derivatives with Respect to Crystal Shape Parameters. *J. Appl. Crystallogr.* **1991**, *24*, 1035−1041.
(90) Sheldrick, G. M. Crystal Structure Refinement with SHELXL. *Acta Crystallogr., Sect. C: Struct. Chem.* **2015**, *71*, 3−8.

DOI: 10.1021/acsomega.9b00365
ACS Omega 2019, 4, 10231−10242